Received: December 22, 2020. Revised: February 26, 2021. 177

International Journal of
Intelligent Engineering & Systems

http://www.inass.org/

Improved Direct Torque Control of Doubly Fed Induction Motor Using Space Vector Modulation

Mohammed El Mahfoud[1]* Badre Bossoufi[1] Najib El Ouanjli[2]
Mahfoud Said[2] Mohammed Taoussi[2]

[1]*Laboratory of engineering Modeling and Systems Analysis, SMBA University Fez, Morocco*
[2]*Technologies and Industrial Services Laboratory, SMBA University Fez, Morocco*
* Corresponding author's Email: Mahfoudmohammed.el@usmba.ac.ma

Abstract: This research paper deals with the improved direct torque control (DTC) of a doubly fed induction machine (DFIM) operating in motor mode. The conventional DTC is a powerful tool to ensure robustness and good torque dynamics. However, the variable switching frequency as well as the presence of torque and flux ripples due to the use of hysteresis controllers are the major drawbacks of this strategy. For this purpose, the control by space vector Modulation (SVM) is developed to improve DTC performance, by replacing hysterisis controllers by PI controllers to reduce electromagnetic flux ripple and torque ripple in order to minimize mechanical vibration and acoustic noise while maintaining the benefits of DTC control. The proposed control algorithm is simulated and tested in MATLAB/Simulink. A comparative analysis between this technique and conventional DTC is carried out, highlighting the efficiency of the proposed improvement approach. The performance indexes and comparative results show the effectiveness of the proposed control in reducing torque ripple and stator and rotor flux ripple by up to 43%, 42% and 31%, respectively, resulting in Total Harmonic Distortion (THD%) 61% lower, in addition the switching frequency is controlled, and the Rejection Time is improved by more than 76%.

Keywords: Direct torque control, Space vector modulation, Doubly fed induction motor, Inverter, Switching table.

1. Introduction

Over the past few decades, drive systems have been used regularly in a number of applications, such as marine propulsion, rail traction, pumping and electric vehicles [1], as well as in hydroelectric and wind power conversion systems [2]. Among these drives, the Doubly Fed Induction Machine (DFIM) presents great robustness, high efficiency, reliability and longevity. Increasing interest is being given to DFIM [3].

Despite its advantages, yet DFIM is still complicated and difficult to control particularly when good performance is required in various operating conditions [4]. This is because DFIM is a non-linear system, multivariable, time-varying and subject to perturbations. In addition, some of its state variables, like flux are not measurable [5]. These constraints require more powerful algorithms to control this machine. The invention of the Field Oriented Control (FOC) algorithm in the 1972s has revived the applications of high-performance variable speed drives [6]. FOC provides decoupling between torque and machine flux and makes the DFIM like a DC machine [7]. This decoupling gives fast torque response, a wide speed control range and high efficiency over a wide load variation range. But this control presents a high sensitivity to the parametric variations of the machine and a great complexity caused by the presence of coordinate transformations and the use of several control variables [8]. In opposition to FOC, Direct Torque Control (DTC) is known by its simple decoupled scheme which allows controlling the electromagnetic flux and torque. DTC offers advantages such as fast response and less dependence on machine parameters. In addition, it does not require any transformation of coordinates or current regulator loops [5]. The DTC has been made

by TAKAHASHI [9]. It is based on the direct application of a control sequence to the switches of the voltage inverter placed before the induction machine {Formatting Citation}. The choice of this sequence is based on the use of a switching table and hysteresis controllers which have the role of controlling and regulating the electromagnetic torque and flux of the machine. However, this technique causes [5]:

- Undesirable flux and torque ripples.
- High and uncontrollable switching frequency.
- Acoustic noise and mechanical vibration of the motor.
- Problems at low speeds.

In recent years, research has been conducted to overcome the drawbacks previously mentioned [1, 11-13]. In [11], A DTC improved by the sliding mode command is studied. This technique provides a good improvement and guarantees robustness against external disturbances and parametric variations of the motor, but there is the problem of the chattering phenomenon which is degrading the performance of the system. The paper [1] presents direct torque control of a DFIM by a PI controller tuned using a genetic algorithm. the GA is a particular class of evolutionary algorithms using techniques inspired by evolutionary biology, which has become a tool for the optimization of nonlinear problems, the major advantage of GA focuses on the optimization of the variable parameters of the system, but which requires a large number of iterations for the system to converge towards optimal solutions. Another method of improving DTC is proposed in [12]. New switching tables are developed using fuzzy logic controllers (FLC) to control the switching frequency. Furthermore, the authors of [13] are proposed another structure of DTC based on the artificial neural network (ANN) to have fast responses of flux and torque with less distortion. However, these last two solutions present a high complexity of design and implementation. For the FLCs, The design and choice of structure is difficult due to the lack of a clear methodology. These techniques of artificial intelligence are not recommended for optimizing excessively complex or very large problems, and requires much time to fine tune all parameters.

Our contribution in this work consists of proposing an improvement of the performances of the classical DTC control for a DFIM operating in motor mode, while keeping its advantages. They are as follows: robustness, simplicity and good speed tracking. The integration of the SVM to the classical DTC is a very attractive solution to guarantee an optimal regulation of the motor under study [14]. For this purpose, the DTC-SVM control strategy (without the use of hysteresis controllers) is recommended, in order to obtain a selection table allowing the best choice of the voltage vector sequence to be applied to the motor, while respecting the constraints on flux and electromagnetic torque [15]. This allows us to directly control the torque without using hysteresis controllers and therefore a significant reduction in the ripple of the control quantities as well as a control of the switching frequency. The behavior of the DFIM controlled by DTC-SVM is evaluated and compared with that of the conventional DTC to highlight the effectiveness of the proposed improvement approach.

This article is divided into six major sections as follows: Section 2 presents a brief modeling of the doubly fed induction machine. Section 3 is devoted to the study of the direct torque control of the DFIM and the explanation of the principle of flux control, electromagnetic torque and the general structure with two switch tables. The modifications made to the DTC control and the principle of space vector modulation is described in section 4. Section 5 shows the results of the simulation of the proposed control techniques, the comparative study between these two control structures is given and discussed. Finally, section 6 presents the conclusion and perceptual considerations.

2. Modeling of the DFIM

The system studied is composed of a doubly fed induction motor associated with two variable frequency power supply systems; one is connected to the stator and the other one to the rotor [16]. Fig. 1 shows the DFIM power supply scheme.

The stator and rotor voltage of DFIM in synchronously rotating reference frame (α, β) can be expressed as [17]:

$$\begin{bmatrix} v_{s\alpha} \\ v_{s\beta} \\ v_{r\alpha} \\ v_{r\beta} \end{bmatrix} = \begin{bmatrix} R_s & 0 & 0 & 0 \\ 0 & R_s & 0 & 0 \\ 0 & 0 & R_r & 0 \\ 0 & 0 & 0 & R_r \end{bmatrix} \begin{bmatrix} i_{s\alpha} \\ i_{s\beta} \\ i_{r\alpha} \\ i_{r\beta} \end{bmatrix} + \frac{d}{dt} \begin{bmatrix} \psi_{s\alpha} \\ \psi_{s\beta} \\ \psi_{r\alpha} \\ \psi_{r\beta} \end{bmatrix} \frac{d\theta}{dt} \begin{bmatrix} 0 \\ 0 \\ -\psi_{r\beta} \\ \psi_{r\alpha} \end{bmatrix} \quad (1)$$

The expression of stator and rotor flux in diphase reference frame (α, β):

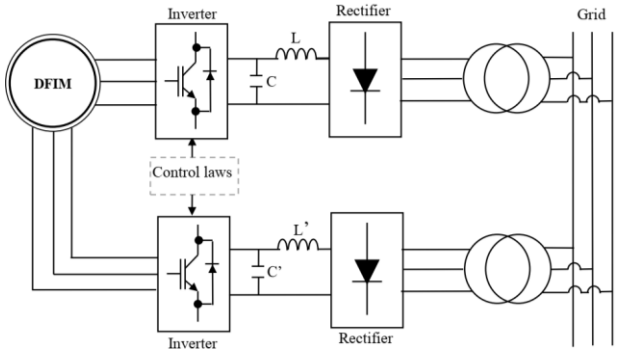

Figure.1 Power system of the DFIM

$$\begin{bmatrix}\psi_{s\alpha}\\ \psi_{s\beta}\\ \psi_{r\alpha}\\ \psi_{r\beta}\end{bmatrix} = \begin{bmatrix} L_s & 0 & M\cos\theta & -M\sin\theta \\ 0 & L_s & M\sin\theta & M\cos\theta \\ M\cos\theta & M\sin\theta & L_r & 0 \\ -M\sin\theta & M\cos\theta & 0 & L_r \end{bmatrix}\begin{bmatrix} i_{s\alpha}\\ i_{s\beta}\\ i_{r\alpha}\\ i_{r\beta}\end{bmatrix} \quad (2)$$

The electromagnetic torque can be determined from:

$$T_{em} = \frac{3}{2}\frac{PM}{\sigma L_s L_r}(\psi_{s\beta}\psi_{r\alpha} - \psi_{s\alpha}\psi_{r\beta}) \quad (3)$$

With: $T_{em} = T_r + J\frac{d\Omega}{dt} + f.\Omega$ (4)

3. Direct torque control strategy

3.1 Principe of the DTC

The DTC aims directly at controlling the torque and flux produced by the machine, without current control, as is the case in the FOC. DTC has many advantages such as less dependence on machine parameters, simpler implementation and a relatively faster dynamic torque response to field-oriented rotor control [18].

Direct torque control allows decoupled control of flux and electromagnetic torque in the reference frame (α, β). It uses a switching table for the selection of a suitable voltage vector [5]. The selection of the switching states is directly related to the variation of the flux and torque of the motor. Therefore, the selection is made by limiting both the flux and torque amplitudes in two hysteresis bands. These controllers provide separate control of these two magnitudes. The inputs of the hysteresis controllers are flux and torque errors, and their outputs determine the appropriate voltage vector for each switching period.

3.2 Application of DTC control to the DFIM

The control must always be asynchronous so at too able to regulate both stator and rotor flux; this means adjusting the torque supplied by the DFIM [12]. The flux expressions are:

$$\begin{cases}\psi_s(t) = \int_0^t (V_s - R_s I_s)dt + \psi_{s0} \\ \psi_r(t) = \int_0^t (V_r - R_r I_r)dt + \psi_{r0}\end{cases} \quad (5)$$

The terms $R_s I_s$ and $R_r I_r$ are considered negligible in front of the voltages $V_s$and V_r. During a sampling period Te, the logic control states (S_A, S_B and S_C) remain fixed. Thus, Eq. (5) becomes:

$$\begin{cases}\Delta\psi_s = \psi_s(k+1) - \psi_s(k) = V_s T_e \\ \Delta\psi_r = \psi_r(k+1) - \psi_r(k) = V_r T_e\end{cases} \quad (6)$$

With:

$\psi(k+1)$: Flux vector (stator or rotor flux) at the next sampling step.

$\psi(k)$: Flux vector (stator or rotor) at the current sampling step.

$\Delta\psi$: Variation of the flux vector $(\psi(k+1) - \psi(k))$.

T_e : Sampling period.

From Eq. (6), it can be noticed that over a sampling interval $[0.T_e]$, the extremity of the flux vector moves on a straight line whose direction is given by the selected voltage vector V for a period T_e, through choosing an appropriate sequence of the voltage vector of the inverter over successive sampling periods of duration T_e. This allows the tracking of the extremity of the flux vector ψ according to the desired trajectory as shown in Fig. 2. The torque expression can be presented as follows:

$$T_{em} = K\|\overrightarrow{\psi_s}\|.\|\overrightarrow{\psi_r}\|.sin\gamma \quad (7)$$

With: K constant depends on motor parameters

$$K = \frac{3}{2}\frac{PM}{\sigma L_s L_r}$$

$$\begin{cases}\|\overrightarrow{\psi_s}\| = \sqrt{\psi_{s\alpha}^2 + \psi_{s\beta}^2} \\ \|\overrightarrow{\psi_s}\| = \sqrt{\psi_{s\alpha}^2 + \psi_{s\beta}^2}\end{cases} \quad (8)$$

$$\gamma = \theta_s - \theta_r \quad (9)$$

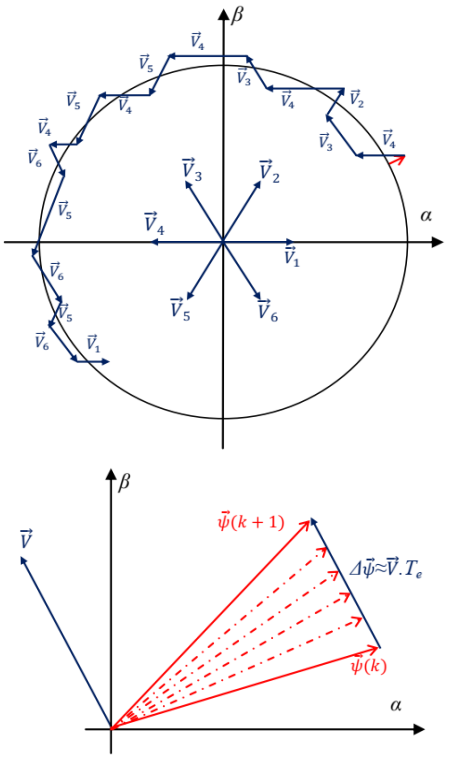

Figure.2 Flux vector evolution

$$\begin{cases} \theta_s = \angle\overrightarrow{\psi_s} = arctg\left(\frac{\psi_{s\beta}}{\psi_{s\beta}}\right) \\ \theta_r = \angle\overrightarrow{\psi_r} = arctg(\frac{\psi_{r\beta}}{\psi_{r\beta}}) \end{cases} \quad (10)$$

This equation shows that the electromagnetic torque depends on the amplitude of the two flux vectors (ψ_s and ψ_r) and their relative position γ. When stator and rotor flux are kept constant, by limiting the flux in hysteresis bands around its set-points, the electromagnetic torque will be a function of the angle of phase shift γ between these fluxes.

In order to act on this angle, the position of the stator flux vector in the frame (α, β) must be varied via applying an appropriate tension vector. In this way, to maximize the value of the torque, it suffices to apply a voltage whose vector is in advanced quadrature with respect to the stator flux vector. Conversely, a reduction of the motor torque in algebraic value can be obtained quickly by applying a voltage vector having a strong delay quadrature component Fig. 3).

The different selection strategies for each voltage vector V are developed from the rules for the evolution of the flux modulus and the electromagnetic torque of the doubly fed induction machine, taking into account information on the position of the flux vector in the complex plane (α, β). To delimit the flux space, a partition into six zones (sectors) of 60˚ of this space is necessary. In

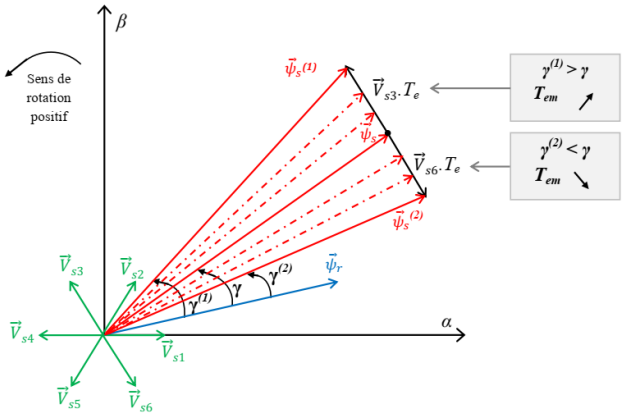

Figure. 3 Electromagnetic torque evolution

Table 1. Choice of voltage vector

	Increase	Decrease
ψ_s or ψ_r	V_{i+1}, V_{i-1}	V_{i+2}, V_{i-2}
T_{em}	V_{i+1}, V_{i+2}	V_{i-1}, V_{i-2}

general, when the flux (stator or rotor) is in the S_i sector, the torque and flux control can be done as presented in Table 1.

The selection of the voltage vector is deduced from the estimated torque and flux deviations from their references, as well as the sector or position where the flux vector was located.

a) Flux controller:

The objective of this controller is to keep the extremity of the flux vector within a circular band as shown in Fig. 4. Two-level hysteresis comparators are used for the correction of stator and rotor flux. The output of each comparator must indicate the direction of evolution of the flux module, to select the corresponding voltage vector.

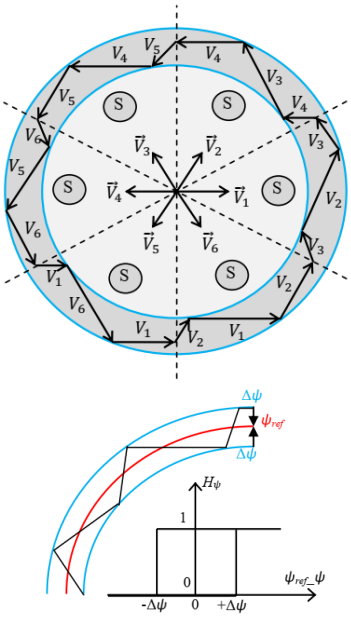

Figure. 4 Flux trajectories

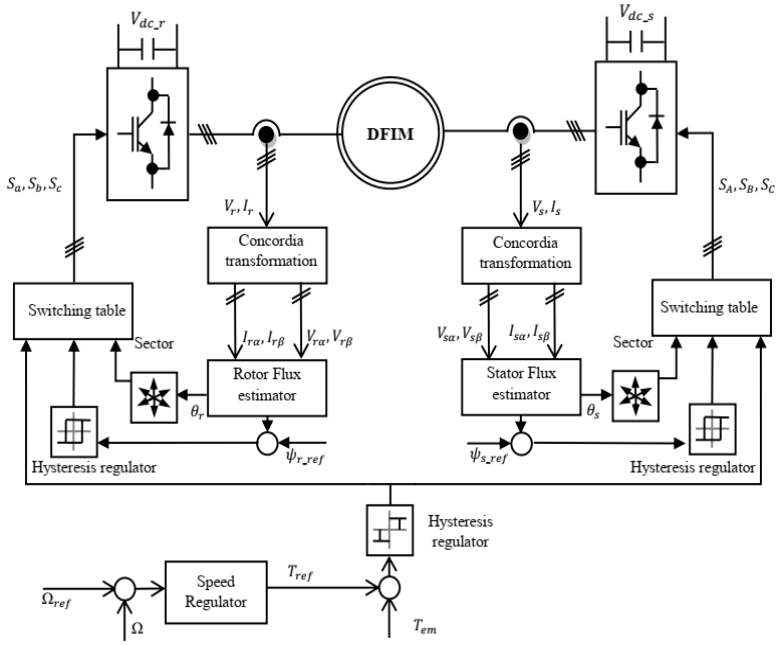

Figure. 5 General structure of DTC of the DFIM

The error between the reference flux and the estimated flux is injected into a two-level hysteresis controller which generates at its output the boolean variable H_ψ, this variable directly indicates whether the flux amplitude should be increased ($H_\psi = 1$) or decreased ($H_\psi = 0$) in order to keep the error between the estimated and reference flux within a hysteresis width $\Delta\psi$ and the inequation $|\psi_{ref} - \psi_{est}| \leq \Delta\psi$ should be checked. If $\varepsilon > \Delta\psi$ or $\varepsilon < -\Delta\psi$, it means the flux is coming out of the hysteresis band. In the first case, it is necessary to impose a voltage vector which increases the flux modulus. In the second case, a voltage vector is imposed which reduces the flux modulus.

b) Electromagnetic torque controller:

For torque correction, a three-level hysteresis comparator is used to control the machine in both directions of rotation. Its role is to keep the electromagnetic torque within the limits $|T_{em_{ref}} - T_{em_{est}}| \leq \Delta T_{em}$. The error $\varepsilon(T_{em}$, between esteemed and reference torque is introduced into a three-level hysteresis comparator, the latter generates at its output the boolean variable H_{Tem}, this variable directly indicates whether the torque amplitude must be increased in absolute value ($H_{T_{em}} = 1$ for a positive set-point and $H_{T_{em}} = -1$ for a negative setpoint) or decreased ($H_{T_{em}} = 0$).

The two voltage inverters supplying the doubly fed induction motor are controlled by a control law generated from two switching tables. Each table is used to select the appropriate voltage vector at each sampling instant according to the state of the boolean variables (H_ψ et H_{Tem}) at the output of the two flux correctors and the electromagnetic torque, as well as the S_i sector giving information on the position of the flux vector in the reference frame (α, β), it is presented in Table 2.

Table 2. Switching table

Flux		0			1		
Torque		-1	0	1	-1	0	1
Sectors	1	V_5	V_0	V_3	V_6	V_7	V_2
	2	V_6	V_7	V_4	V_1	V_0	V_3
	3	V_1	V_0	V_5	V_2	V_7	V_4
	4	V_2	V_7	V_6	V_3	V_0	V_5
	5	V_3	V_0	V_1	V_4	V_7	V_6
	6	V_4	V_7	V_2	V_5	V_0	V_1

Fig. 5 illustrates the general structure of direct torque control of the doubly fed induction motor connected by two voltage inverters.

4. Direct torque control based on space vector modulation

4.1 Principe of the DTC

The main disadvantages of conventional direct torque control are the variable switching frequency and the high level of ripples. Consequently, they cause high current harmonics, acoustic noise and degrade the performance of the control particularly at low speed [19]. The ripples are proportionally affected by the width of the hysteresis band. However, even when choosing lower bandwidth values, the ripples remain large due to the discrete nature of

hysteresis controllers. In addition, very small bandwidth values increase the switching frequency of the inverter [12].

DTC-SVM for DFIM control powered by two inverters includes three PI controllers for regulating torque and stator and rotor flux. The torque PI controller generates the quadratic stator and rotor voltage V_q ,thus the output of the two other PI controllers in the flux loop gives the voltages directsV_d.Once V_d and V_q are obtained, they must be transformed to a fixed reference (α, β) which are both inputs delivered to space the vector modulator (SVM),which generates switching signals S_A, S_B, S_C for the power transistors of the inverters [20].

4.2 Application of DTC control to the DFIM

The SVM is different from conventional pulse-width modulation (PWM). It is based on the vectorial spatial representation of the inverter output. There are no separate modulators for each phase. The reference voltages are given by the spatial voltage vector (i.e. the components of the voltage vector in the complex plane) [21]. The principle of SVM is the prediction of the inverter voltage vector by projecting the reference vector V_{ref} between adjacent vectors corresponding to two non-zero switching states [22]. For a two-level inverter, the switching vector diagram forms a hexagon divided into six sectors, each expanded by 60° as shown in Fig. 6.

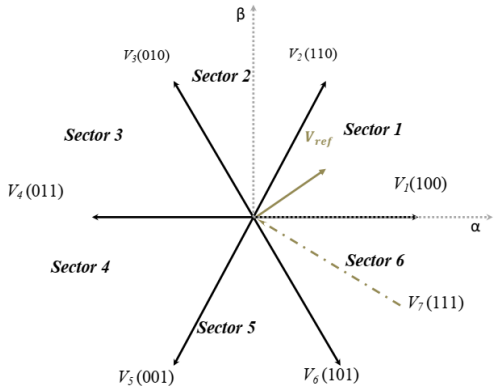

Figure. 6 Diagram of voltage space vector

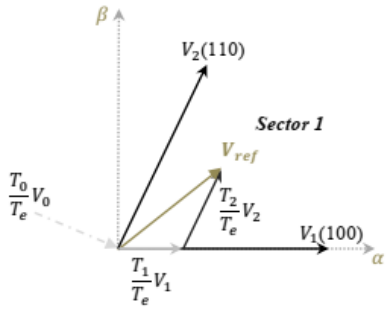

Figure. 7 Reference vector as a combination of adjacent vectors at sector 1

Table 3. Inverter switch control signals

Sector1	$T_1 = -Z, T_2 = X$
Sector2	$T_2 = Y, T_3 = Z$
Sector 3	$T_3 = X, T_4 = -Y$
Sector 4	$T_4 = Z, T_5 = -X$
Sector 5	$T_5 = -Y, T_6 = -Z$
Sector 6	$T_6 = -X, T_1 = Y$

The application time for each vector can be obtained by vector calculations and the rest of the time period will be spent by applying the zero vector [23].

When the reference voltage is in sector 1 (Fig. 7), the reference voltage can be obtained by synthesis using the vectors V_1, V_2 and V_0 (zero vector). The volt-second principle for sector 1 can be expressed by:

$$V_{ref}T_e = V_1T_1 + V_2T_2 + V_0T_0 \quad (11)$$

$$T_e = T_1 + T_2 + T_0 \quad (12)$$

T_1, T_2 and T_0 are the corresponding application times of the voltage vectors.

The determination of the times T_1 and T_2 which correspond to the voltage vectors is obtained by simple projections:

$$T_1 = \frac{T_e}{2V_{dc}}\left(\sqrt{6}V_\beta - \sqrt{2}V_\alpha\right) \quad (13)$$

$$T_2 = \frac{T_e}{V_{dc}}\sqrt{2}V_\alpha \quad (14)$$

The method already presented for V_{ref} between V_1 and V_2 is redone for the sectors. Table 3 shows the different application times of the state vectors for the different sectors (S_1 to S_6) from the values of the following variables X, Y and Z:
With:

$$X = \frac{T_e}{V_{dc}}\sqrt{2}V_\alpha \quad (15)$$

$$Y = \frac{T_e}{2V_{dc}}\left(\sqrt{6}V_\beta + \sqrt{2}V_\alpha\right) \quad (16)$$

$$Z = \frac{T_e}{2V_{dc}}\left(\sqrt{2}V_\alpha - \sqrt{6}V_\beta\right) \quad (17)$$

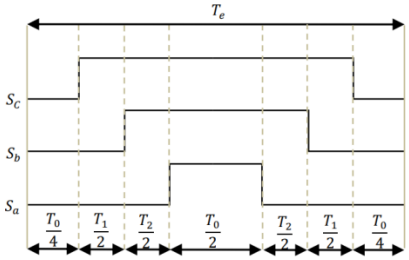

Figure. 8 Switching times of sector 1

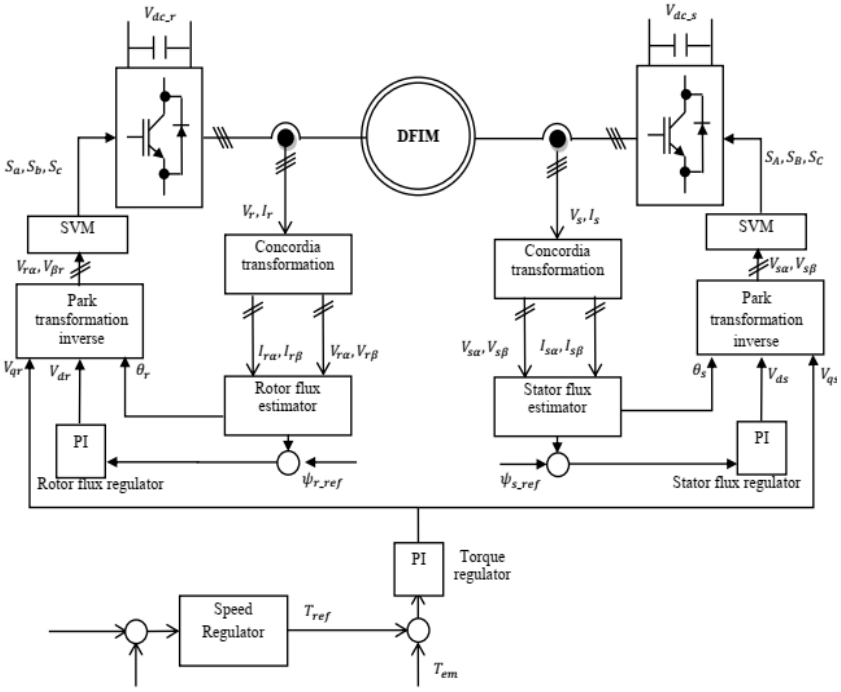

Figure. 9 Block diagram DTC-SVM scheme for DFIM drive

The calculation of the switching times (duty cycles) is expressed as follows:

$$T_{aon} = \frac{T_e - T_1 - T_2}{2} \quad (18)$$

$$T_{bon} = T_{aon} + T_1 \quad (19)$$

$$T_{con} = T_{bon} + T_2 \quad (20)$$

The carrier wave generated by the SVM model is symmetrical. An example for this wave with a period T_e in sector 1 is illustrated in Fig. 8.

Fig. 9 illustrates the general structure of DTC-SVM control of the doubly fed induction motor connected by two voltage inverters.

5. Simulation results

In this section, the conventional DTC and SVM-DTC controls of the doubly fed induction motor have been tested by simulation under the MATLAB/Simulink environment. The motor parameters are mentioned in the appendix.

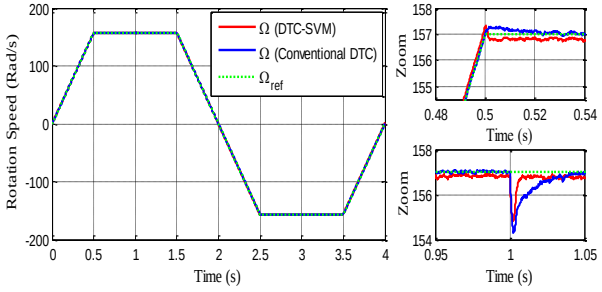

Figure. 10 Rotation speed

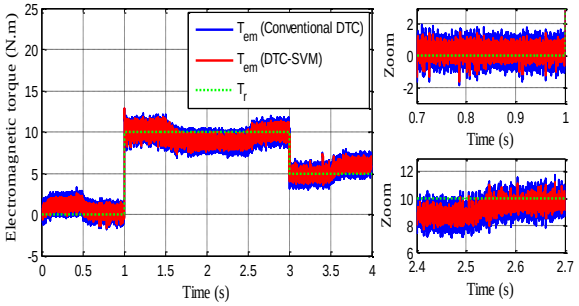

Figure. 11 Electromagnetic torque

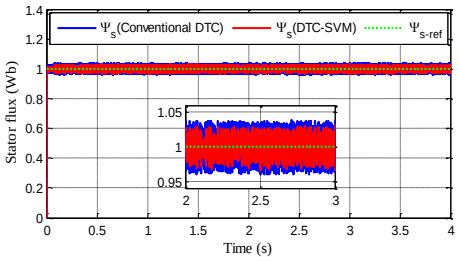

Figure. 12 Stator flux

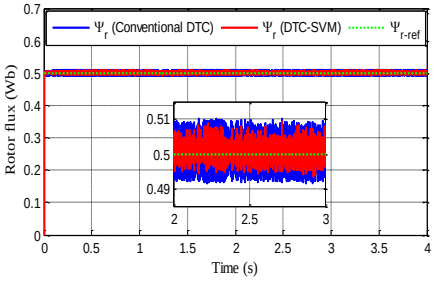

Figure. 13 Rotor flux

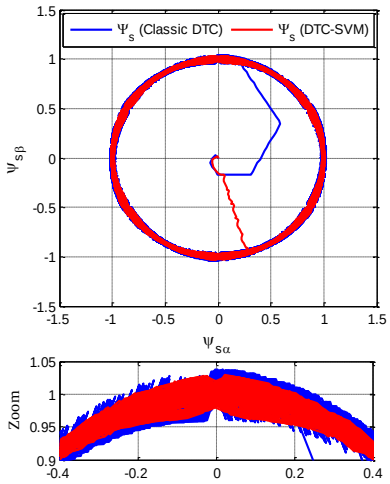

Figure.14 Stator flux evolution

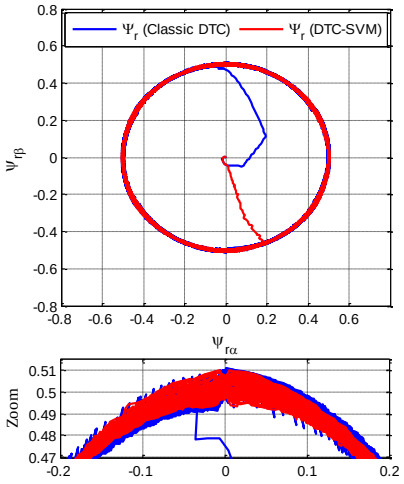

Figure.15 Rotor flux evolution

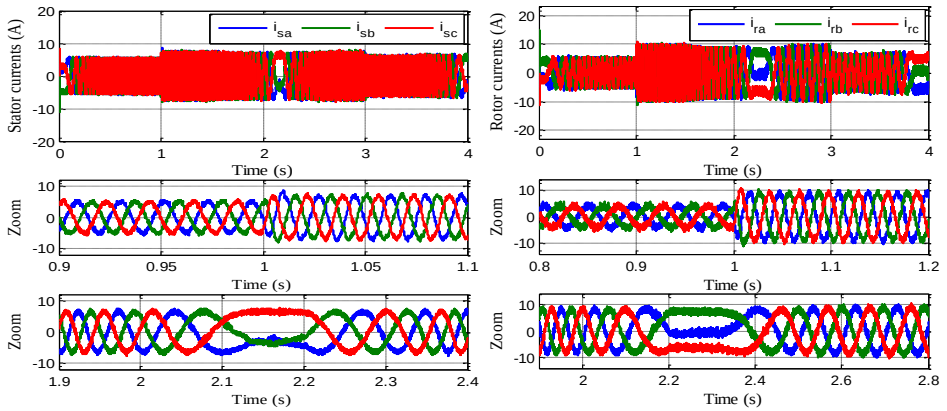

Figure. 16 Stator and rotor current by conventional DTC

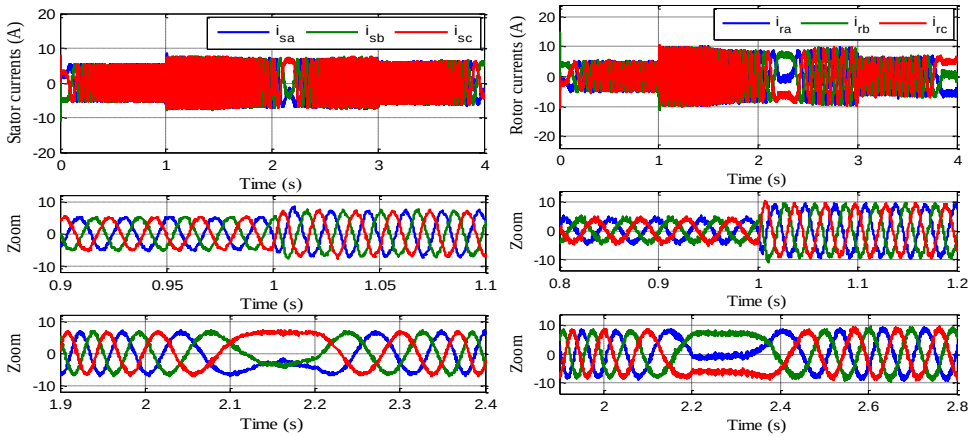

Figure. 17 Stator and rotor current by DTC-SFM

The following figures show the simulation results obtained for a trapezoidal speed set-point with reversal of rotation direction. By applying a load torque of 10 N.m and 5 N.m to $t_1 = 1s$ and $t_2 = 3s$.

6. Discussion

The results obtained show that the DTC-SVM control presents satisfactory results with a good tracking dynamic. The rotation speed relatively follows its reference (Fig. 10). The reference torque, load torque and the motor torque are shown in Fig. 11. In this case, the load torque is considered a disturbance. As the startup is empty, the motor torque returns practically to zero at the end of the transient regime. However, at the instant of overloading the motor, a drop in speed is caused; this disturbance is quickly rejected (10ms for DTC-SVM and for 42ms

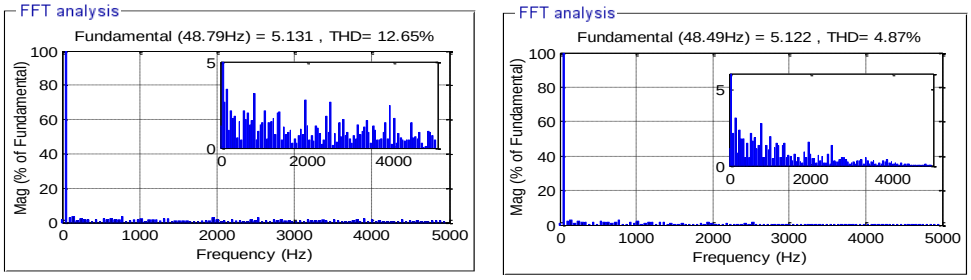

(a) (b)

Figure. 18 Harmonic analysis of rotor current spectra by control: (a) conventional DTC and (b) DTC-SVM

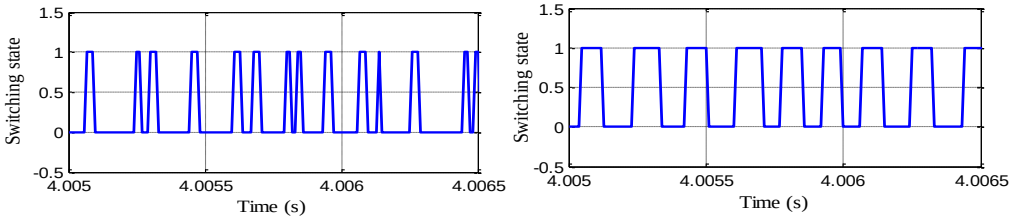

(a) (b)

Figure. 19 Switching stats Sa by control: (a) conventional DTC and (b) DTC-SVM

Table 4. Comparison between conventional DTC and DTC-SVM

Performance	Conventional DTC	DTC-SVM	Improvement (%)
Torque ripple (N.m)	2.92	1.64	43.83
Stator flux ripple (Wb)	0.089	0.051	42.69
rotor flux ripple (Wb)	0.0175	0.012	31.42
THD of the phase current i_{sa} (%)	12.65	4.87	61.50
Speed rejection time	42ms	10 ms	76.19
Switching frequency	Variable frequency of 8.66 kHz	Almost constant frequency of 5.62KHz	Switching frequency is mastered

Table 5. Comparison of our proposal with some published controls strategy

Publication reference	Method	Response time (s)	Torque Ripple (N.m)	Complexity	Robustness
[24]	Sliding mode control	0.19	2.40	high	Not robust
[1]	GA based DTC	0.18	0.16	Very high	Robust
[12]	Fuzzy based DTC	0.28	1.14	Very high	Robust
Proposal Method	DTC-SVM	0.16	1.64	Medium	Robust

conventional DTC). Moreover, the electromagnetic torque by DTC-SVM presents fewer ripples compared to that of conventional control.

Figs.12 and 13 show that the stator and rotor flux modules follow its references (1Wb for the stator flux and 0.5Wb for the rotor flux). But these flux by conventional DTC have ripples compared to DTC-SVM due to the use of hysteresis comparators, they are not affected by the variation in load and speed (Figs. 14 and 15). The components of the rotor and stator currents for both techniques are presented in Figs. 16 and 17. They respond well to the variations imposed by the load torque. They have a sinusoidal shape.

Furthermore, Fig. 18 shows the spectral analysis of the stator current "i_{sa}" absorbed by the DFIM. The total harmonic distortion (THD) of phase current by the DTC-SVM control is considerably reduced compared to conventional DTC.

Fig. 19 illustrates the switching state of the "S_a" switch for the two control strategies. The switching frequency obtained by DTC-SVM is lower than that of conventional DTC, and so reducing switching losses.

Table 4 summarizes the comparative study between the two controls in terms of speed tracking, torque ripples, flux ripples and spectral harmonic analysis of currents and switching frequency.

A comparison between the proposed technique and some published control strategies is presented in Table 5. It should be noted that they do not refer to the same conditions since it is very difficult to find

several works carried out under the same conditions. Therefore, if we compare the proposed works with the sliding mode [24], our solution has a faster response and reduced torque ripples. In addition, our system is insensitive to load torque variations, which demonstrates a high level of robustness a high level of robustness. Thus, DTC using PI controller tuned using genetic algorithm presented by [1] and the fuzzy DTC presented by [12] presents less torque ripples than our proposal, but these controls are very complex for this reason fast processors are used, which leads to an increase in the cost of the system.

7. Conclusion

This paper has presented a direct torque control scheme based on space vector modulation for doubly fed induction motor powered by two voltage inverters. The objective is to improve the performance of conventional DTC. The dynamic model of DFIM and the principle of DTC strategies have been presented. The control technique DTC based on space vector modulation is developed in detail. After testing the system controls using MATLAB/SIMULINK, the key findings of this work are as follows:

- Space Vector Modulation (SVM) is an efficient method of improving DTC. Flux and torque ripples are minimised by 43% and 42% respectively. Consequently, fewer problems for DFIM are caused, such as ageing, mechanical vibrations, heating…
- Compared to traditional DTC, the proposed technique optimises the harmonic distortion of the rotor and stator currents by 61%.
- The fast response, torque dynamics and robustness merits of the classic DTC are preserved.

The future work will address the experimental validation of DTC-SVM control using the dSPACE DS1104 platform.

APPENDIX

PARAMETERS OF THE DFIM

Variable	Symbol	Value (unit)
Nominal power	P_m	1.5 kW
Frequency	f	50 Hz
Pair pole number	P	2
Stator resistance	R_s	1.75 Ω
Rotor resistance	R_r	1.68 Ω
Mutual inductance	M	0.165 H
Stator self-inductance	L_s	0.295 H
Rotor self-inductance	L_r	0.104 H
Total inertia	J	0.01 Kg.m²
Total viscous frictions	f	0.0027 Kg.m²/s

NOMENCLATURES:

$\psi_{r(\alpha,\beta)}$, $\psi_{r(\alpha,\beta)}$	:Rotor and stator flux in (α,β) reference.
$V_{r(\alpha,\beta)}$,$v_{s(\alpha,\beta)}$	:Rotor and stator voltages in (α,β) reference.
$i_{r(\alpha,\beta)}$, $i_{s(\alpha,\beta)}$	:Rotor and stator currents in (α,β) reference.
S_A , S_B, S_C	: Switching states.
R_r, R_s	: Rotor and stator resistances.
M	: Mutual inductance.
L_r, L_s	: Rotor and stator inductances.
J	: Moment of inertia.
f	: Coefficient of viscous friction.
p	: Number of pole pair.
ω_r, ω_s	: Rotor and stator pulsations.
ω	: Mechanical pulsation.
Ω	: Rotation speed.
T_r , T_{em}	: Load and Electromagnetic torque.
θ_r, θ_s	: Position of the rotor and stator flux.
V_{DC}	: DC bus voltage.
γ	: Angle between the two rotor and stator flux vectors.
T_e	: Sampling period.

ABBREVIATIONS:

ANN	: Artificial Neural Network
DTC	: Direct Torque Control.
DFIM	: Doubly Fed Induction Machine.
FOC	: Field Oriented Control.
FLC	: Fuzzy Logic Controller
SVM	: Space Vector Modulation.
THD	: Total Harmonics Distortion.

Conflicts of Interest

The authors declare no conflict of interest.

Author Contributions

Conceptualization by Mohammed El Mahfoud and Najib El Ouanjli; methodology, Mohammed Taoussi; software, Mahfoud Said; validation, resources, and formal analysis by Badre Bossoufi; writing—original draft preparation, Mohammed El Mahfoud and Mahfoud Said; writing—review and editing, Najib El Ouanjli and Mohammed Taoussi; visualization, supervision and project administration by Badre Bossoufi.

References

[1] A. Zemmit, S. Messalti, and A. Harrag, "A new improved DTC of doubly fed induction machine using GA-based PI controller", *Ain Shams Engineering Journal*, Vol. 9, No. 4, 1877-1885, 2018.

[2] S. Boubzizi, H. Abid, and M. Chaabane, "Comparative study of three types of controllers for DFIG in wind energy conversion system", *Protection and Control of Modern Power Systems*, Vol. 3, No. 1, pp. 21, 2018.

[3] B. Bossoufi, M. Karim, A. Lagrioui, M. Taoussi, and A. Derouich, "Observer backstepping control of DFIG-Generators for wind turbines variable-speed: FPGA-based implementation", *Renewable Energy*, Vol. 81, pp. 903-917, 2015.

[4] M. Taoussi, M. Karim, D. Hammoumi, C. El Bekkali, B. Bossoufi, and N. El Ouanjli, "Comparative study between Backstepping adaptive and Field-oriented control of the DFIG applied to wind turbines", In: *Proc. of IEEE International Conf. on Advanced Technologies for Signal and Image Processing*, pp. 1-6, 2017.

[5] N. El Ouanjli, A. Derouich, A. El Ghzizal, A. Chebabhi, and M. Taoussi, "A comparative study between FOC and DTC control of the Doubly Fed Induction Motor (DFIM)", In: *Proc. of* E*EE International Conf. on Electrical and Information Technologies*, pp. 1-6, 2017.

[6] M. Yano, S. Abe, and E. Ohno, "History of power electronics for motor drives in Japan", In: *Proc. of IEEE Conf. on the History of Electronics*, pp. 1-11, 2004.

[7] D. A. Dominic and T. R. Chelliah, "Analysis of field-oriented controlled induction motor drives under sensor faults and an overview of sensorless schemes", *ISA Transactions*, Vol. 53, No. 5, pp. 1680-1694, 2014.

[8] R. Kumar, S. Das, and A. Bhaumik, "Speed sensorless model predictive current control of doubly-fed induction machine drive using model reference adaptive system", *ISA Transactions*, Vol. 86, pp. 215-226, 2019.

[9] I. Takahashi and T. Noguchi, "A new quick-response and high-efficiency control strategy of an induction motor", *In IEEE Transactions on Industry Applications*, Vol. 5, pp. 820-827, 1986.

[10] T. Sutikno, N. R. N. Idris, and A. Jidin, "A review of direct torque control of induction motors for sustainable reliability and energy efficient drives", *Renewable and Sustainable Energy Reviews*, Vol. 32, pp. 548-558, 2014.

[11] D. Mehmet, "Sensorless sliding mode direct torque control (DTC) of induction motor", In: *Proc. of the IEEE International Symposium on Industrial Electronics*, 2005.

[12] N. El Ouanjli, S. Motahhir, A. Derouich, A. El Ghzizal, A. Chebabhi, and M. Taoussi, "Improved DTC strategy of doubly fed induction motor using fuzzy logic controller", *Energy Reports*, Vol. 5, pp. 271-279, 2019.

[13] A. Zemmit, S. Messalti, and A. Harrag, "Innovative improved direct torque control of doubly fed induction machine (DFIM) using artificial neural network (ANN-DTC)", *International Journal of Applied Engineering Research*, Vol. 11, No. 16, pp. 9099-9105, 2016.

[14] T. G. Habetler, F. Profumo, M. Pastorelli, and L. M. Tolbert, "Direct torque control of induction machines using space vector modulation", *IEEE Transactions on Industry Applications*, Vol. 28, No. 5, pp. 1045-1053, 1992.

[15] A. Ammar, A. Bourek, and A. Benakcha, "Nonlinear SVM-DTC for induction motor drive using input-output feedback linearization and high order sliding mode control", *ISA Transactions*, Vol. 67, pp. 428-442, 2017.

[16] M. EL Mahfoud, B. Bossoufi, M. Taoussi, N. El Ouanjli, and A. Derouich, "Rotor Field Oriented Control of Doubly Fed Induction Motor", In: *Proc. of IEEE 5th International Conf. on Optimization and Applications*, pp. 1-6, 2019.

[17] G. Abad, J. Lopez, M. Rodriguez, L. Marroyo, and G. Iwanski, "Doubly fed induction machine: modeling and control for wind energy generation", *John Wiley & Sons*, Vol. 85, 2011.

[18] B. L. G. Costa, C. L. Graciola, B. A. Angélico, A. Goedtel, and M. F. Castoldi, "Metaheuristics optimization applied to PI controllers tuning of a DTC-SVM drive for three-phase induction motors", *Applied Soft Computing*, Vol. 62, pp. 776-788, 2018.

[19] H. Mesloub, R. Boumaaraf, M. T. Benchouia, A. Goléa, N. Goléa, and K. Srairi, "Comparative study of conventional DTC and DTC_SVM based control of PMSM motor—Simulation and experimental results", *Mathematics and Computers in Simulation*, Vol. 167, pp. 296-307, 2020.

[20] M. Zelechowski, M. P. Kazmierkowski, and F. Blaabjerg, "Controller design for direct torque controlled space vector modulated (DTC-SVM) induction motor drives", In: *Proc. of the IEEE International Symposium on Industrial Electronics, ISIE*. Vol. 3, pp. 951-956, 2005.

[21] S. K. Barik and K. K Jaladi, "Five-phase induction motor DTC-SVM scheme with PI controller and ANN controller", *Procedia Technology*, Vol. 25, pp. 816-823, 2016.

[22] H. Abu-Rub, D. Stando, and M. P. Kazmierkowski, "Simple speed sensorless DTC-SVM scheme for induction motor drives", *Bulletin of the Polish Academy of*

Sciences, Technical Sciences, Vol. 61, No. 2, 2013.

[23] J. S. Kim and S. K Sul, "A novel voltage modulation technique of the space vector PWM", *IEEJ Transactions on Industry Applications*, Vol. 116, No. 8, pp. 820-825, 1996.

[24] S. Abderazak and N. Farid, "Comparative study between Sliding mode controller and Fuzzy Sliding mode controller in a speed control for doubly fed induction motor", In: *Proc. of 4th International Conf. on Control Engineering & Infonnation Technology*, Tunisia, pp. 16–18, 2016.